Macartney Keir (Orcid ID: 0000-0002-9461-0445)
Lesser Michael (Orcid ID: 0000-0002-0741-3102)

Running Head: Mesophotic Sponge Trophic Ecology

Trophic Ecology of Caribbean Sponges in the Mesophotic Zone

Keir J. Macartney[1], Marc Slattery[2], Michael P. Lesser[1]

[1]University of New Hampshire, Department of Molecular, Cellular and Biomedical Sciences and School of Marine Science and Ocean Engineering, Durham, NH 03824 USA

Corresponding author: kjm1049@wildcats.unh.edu – Keir Macartney (ORCID ID: 0000-0002-9461-0445)

mpl@unh.edu – Dr. Michael Lesser (ORCID ID: 0000-0002-0741-3102)

[2]University of Mississippi, Department of BioMolecular Science, Oxford, MS 38677 USA

slattery@olemiss.edu – Dr. Marc Slattery (ORCID ID: 0000-0001-8325-3262)

Keywords: sponges, stable isotopes, mesophotic, particulate organic material, dissolved organic material, compound-specific isotope analysis, microbiome

This is the author manuscript accepted for publication and has undergone full peer review but has not been through the copyediting, typesetting, pagination and proofreading process, which may lead to differences between this version and the Version of Record. Please cite this article as doi: 10.1002/lno.11668

This article is protected by copyright. All rights reserved.

Author Manuscript

Author Manuscript

Abstract

Sponges are a crucial component of Caribbean coral reef ecosystem structure and function. In the Caribbean, many sponges show a predictable increase in percent cover or abundance as depth increases from shallow (<30 m) to mesophotic (30-150 m) depths. Given that sponge abundances are predicted to increase in the Caribbean as coral cover declines, understanding ecological factors that control their distribution is critical. Here we assess if sponge cover increases as depth increases into the mesophotic zone for three common Caribbean reef sponges, *Xestospongia muta*, *Agelas tubulata* and *Plakortis angulospiculatus*, and use stable isotope analyses to determine whether shifts in trophic resource utilization along a shallow to mesophotic gradient occurred. Ecological surveys show that all target sponges significantly increase in percent cover as depth increases. Using bulk stable isotope analysis, we show that as depth increases there are increases in the $\delta^{13}C$ and $\delta^{15}N$ values, reflecting that all sponges consumed more heterotrophic picoplankton, with low C:N ratios in the mesophotic zone. However, compound-specific isotope analysis of amino acids (CSIA-AA) shows that there are species-specific increases in $\delta^{13}C_{AA}$ and $\delta^{15}N_{AA}$ values. *Xestospongia muta* and *P. angulospiculatus* showed a reduced reliance on photoautotrophic resources as depth increased, while *A. tubulata* appears to rely on heterotrophy at all depths. The $\delta^{13}C_{AA}$ and $\delta^{15}N_{AA}$ values of these sponges also reflect species-specific patterns of host utilization of both POM and dissolved organic matter (DOM), its subsequent re-synthesis, and translocation, by their microbiomes.

Author Manuscript

Introduction

As coral reefs around the world continue to show declines in biodiversity and health (Hoegh-Guldberg et al. 2007, Hughes et al. 2017, 2018) there has been increased interest in understanding processes affecting the structure and function of coral reef communities in the Anthropocene (Waters et al. 2016). The decline in coral cover due to anthropogenic stressors such as pollution, ocean acidification and increases in sea surface temperature (e.g., Hoegh-Guldberg et al. 2007) has resulted in ecological phase shifts in the benthic communities of many coral reefs (McManus et al. 2000). These community shifts are predicted to cause an increase in the abundance of sponges, and changes in the functional attributes of coral reefs as sponge biomass exceeds coral biomass Caribbean-wide (McMurray et al. 2010, Bell et al. 2013, 2018). In the Caribbean, sponges provide an important source of food and habitat for a variety of coral reef species (Diaz & Rutzler 2001, Bell 2008). Sponges also play an important role in benthic food webs through benthic-pelagic coupling due to their consumption of live particulate organic material (POM) (Pile 1997, Lesser 2006, Lesser & Slattery 2013) and dissolved organic material (DOM) (de Goeji et al. 2013, 2017, Mueller et al. 2014), thus coupling water column productivity to benthic secondary productivity (Gili & Coma 1998, Lesser, 2006).

While many ecological studies on the trophic ecology of sponges have been conducted on shallow coral reefs (de Goeij et al. 2017), studies in the mesophotic zone, while increasing (Loya et al. 2016), are not as common (Lesser et al. 2018). The mesophotic zone is found between 30-150 m and is defined primarily by gradients of abiotic factors, particularly irradiance (Lesser et al. 2018). Along the shallow to mesophotic depth gradient, sponges exhibit increased growth rates, abundances, and diversity (Lesser 2006, Trussel et al. 2006, Lesser & Slattery 2013, Slattery & Lesser 2015). Additionally, their primary particulate food sources, auto- and

Author Manuscript

heterotrophic picoplankton, increase with depth (Lesser 2006, Lesser & Slattery 2013). As sponges consume particulate and dissolved food in proportion to its availability (Lesser 2006, de Goeij et al. 2008, Slattery & Lesser 2015), mesophotic sponges should therefore consume more POM with increasing depth (e.g. Slattery and Lesser 2015). Despite the fact that dissolved organic carbon (DOC) declines with increasing depth (Lesser et al. 2019), it has been suggested that carbon, including both particulate organic carbon (POC) and DOC, is not limiting for sponges along the shallow to mesophotic depth range (Lesser et al. 2018, 2020, Lesser & Slattery 2018). Nitrogen, however, is much more likely to be a limiting nutrient for sponge growth (e.g. Hadas et al. 2009). Heterotrophic picoplankton, with low C:N ratios, increase significantly in abundance with increasing depth and may supply the nitrogen required for the increased growth rates and biomass of mesophotic sponges (Lesser et al. 2018). These patterns suggest that sponge populations along the shallow to mesophotic depth gradient are strongly influenced by bottom-up processes (Slattery & Lesser 2015, de Goeij et al. 2017, Wulff 2017, Lesser et al. 2018).

One of the most common analytical tools used for studying the trophic ecology of an organism is bulk stable isotopic analysis (SIA), particularly the stable isotopes $\delta^{15}N$ and $\delta^{13}C$ (Fry 2006). However, sponges present a unique problem for SIA-based studies of their trophic ecology due to the presence of a diverse microbiome in their tissues and their consumption of free-living microbes in the plankton (Hentschel et al. 2012, Pita et al. 2018). For sponges, the bulk $\delta^{13}C$ and $\delta^{15}N$ values increase as depth increases into the mesophotic zone (Slattery et al. 2011, Morrow et al. 2016), indicating a shift in diet from autotrophic to heterotrophic resources in sponge diets at mesophotic depths. Using compound-specific isotope analysis of amino acids (CSIA-AA) may provide increased resolution, compared to bulk SIA, of sponge trophic ecology along environmental gradients. Because of the unique fractionation patterns for stable isotopes of

Author Manuscript

C and N for amino acids (AAs), the $\delta^{13}C$ of essential amino acids (EAAs) can be used to effectively "fingerprint" the biosynthetic origin of source carbon due to the highly conserved modes of carbon acquisition in bacteria, algae and fungi as the $\delta^{13}C$ of these EAA is maintained throughout the food web due to low fractionation between trophic levels (Larsen et al. 2009, 2013, McMahon et al. 2016), which allows for predictions of source end-members utilized by the consumer (Larsen et al. 2013). The $\delta^{15}N$ composition of "source" (e.g. phenylalanine) vs "trophic" (e.g. glutamic acid) AAs are informative for both the estimation of trophic position (TP) and the $\delta^{15}N$ composition of AAs at the base of the food web. Source AAs (SAA) undergo minimal to no fractionation as they are transferred through a food web (Phe = ~ 0.5‰) (Chikaraishi et al. 2009) and thus reflect the biosynthetic origin of that SAA, whereas the $\delta^{15}N$ of trophic AAs (TAA) increase by as much as ~7-8‰ per trophic level (McClelland & Montoya 2002, Chikaraishi et al. 2009, McMahon et al. 2015). Additionally, ΣV values, a measure of bacterial resynthesis and translocation of organic matter, has been successfully used to understand the interactions between the sponge host and its microbiome (Shih et al. 2020). ΣV values assess the reliance of sponges on translocated organic material versus feeding from the water column and will be applied here using the CSIA-AA data on sponges from shallow to mesophotic depths.

Agelas tubulata, Xestospongia muta and *Plakortis angulospiculatus* are three common sponges on coral reefs throughout the Caribbean, and are all classified as high microbial abundance (HMA) sponges (Gloeckner et al. 2014). While HMA sponges are known to filter feed upon picoplankton (e.g., Lesser 2006) it is generally accepted that because of their high microbial densities they efficiently utilize DOM as well (Maldonado et al. 2012). Here we assess if the percent cover of these three sponge species increases as depth increases into the

Author Manuscript

mesophotic zone on Little Cayman Island, and use SIA and CSIA-AA to quantify shifts in trophic resource utilization along a shallow to mesophotic depth gradient. We hypothesize that these sponges will increase in cover with increasing depth and rely upon the increasing concentration of available POM with increasing depth and this will be reflected in their isotopic signatures. Additionally, variability in the utilization of DOM by the sponge microbiome with depth will affect the transfer of re-synthesized organic material to the host, which will be reflected in reductions in the ΣV values of these sponges.

Materials and methods

Target sponge abundance surveys, sample collection and processing

Replicate samples (n = 3) of *Agelas tubulata*, *Xestospongia muta* and *Plakortis angulospiculatus* were collected using open circuit technical diving at 10, 18, 30, 61 and 91 m at Rock Bottom Wall, Little Cayman, Cayman Islands (19º 42'7.36" N, 80º 3'24.94" W) in the Spring of 2009. The abiotic environment (i.e., light, temperature) of this site from shallow to mesophotic depths is described in Morrow et al. (2016), while from an oceanographic perspective this site is occasionally impacted by internal waves (Lesser et al. 2009). To quantify sponge cover with increasing depth the percent cover of the target species was estimated using replicate (n=10) 1 m^2 quadrats positioned at random points along transect lines (n=3-9 at each depth) of 20 x 2 m at each depth. The survey data for *P. angulospiculatus* presented are from Slattery et al. (2016) and reanalyzed for this study. At each depth, all sponges were sampled by cutting a "pie-slice" of sponge tissue from the apical lip of the osculum including both pinacoderm and mesohyl as described in Morrow et al. (2016). Samples were transported on ice to the laboratory and

immediately frozen. All samples were transported frozen to the University of New Hampshire where they were freeze-dried and ground to a powder for stable isotope analyses.

Bulk stable isotope analysis

Bulk stable isotope data for *X. muta* were taken from Morrow et al. (2016), and for *Agelas tubulata* the data are from Slattery et al. (2011) and reanalyzed here to compare to the CSIA-AA analyses. Briefly, subsamples from each piece of sponge tissue, sampled as described above, were sent to the Marine Biological Laboratory (Woods Hole, MA) for the bulk analysis of particulate C and N, as well as the natural abundance of the stable isotopes $\delta^{15}N$ and $\delta^{13}C$. Samples were analyzed using a Europa ANCA-SL elemental analyzer-gas chromatograph attached to a continuous-flow Europa 20-20 gas source stable isotope ratio mass spectrometer. The carbon isotope results are reported relative to Vienna Pee Dee Belemnite, nitrogen isotope results are reported relative to atmospheric air, and both are expressed using the delta (δ) notation in units per mil (‰).

Compound specific isotope analysis of amino acids

Sponge samples were sent to the Isotope Biogeochemistry Laboratory at the University of Hawai‘i at Mānoa for $\delta^{15}N$ and $\delta^{13}C$ analysis of individual amino acids. Both $\delta^{15}N$ and $\delta^{13}C$, were quantified using gas chromatography/combustion-isotope ratio mass spectrometry (GC/C-IRMS) after amino acid extraction and derivatization. Samples were analyzed using either a Thermo Scientific Delta V Plus or a Thermo Scientific MAT 253 mass spectrometer interfaced with a Thermo Finnigan Trace GC gas chromatograph via a Thermo Finnigan GC-C III. The amino acids measured using this technique were alanine (Ala), glycine (Gly), threonine (Thr),

Author Manuscript

Author Manuscript

serine (Ser), valine (Val), leucine (Leu), isoleucine (Iso), proline (Pro), aspartic acid (Asp), phenylalanine (Phe) and lysine (Lys). The terminal amide groups in glutamine (Gln) and aspartame (Asn) were cleaved during the chemical isolation of amino acids. This resulted in the conversion of these amino acids to glutamic acid (Glu) and aspartic acid (Asp), respectively. Thus, the isotope value of the combined Glu + Gln was measured (termed Glx), and the isotope value of a combined Asn + Asp was measured (termed Asx). Averaged AA $\delta^{13}C$ and $\delta^{15}N$ values from these analyses can be found in Tables S1 and S2, while additional information on CSIA is available in the supplemental document.

Statistical analyses

Statistical analyses were conducted using PRIMER (version 7) or JMP (v. 14), and R (version 3.4.3). Differences in percent cover of sponges as a function of depth was assessed with linear regression. Differences in bulk SIA values between species was assessed using ANOVA, and differences between SIA values along the depth gradient were assessed using linear regression.

The $\delta^{13}C$ values of each amino acid in all sponge samples were normalized to the mean value of all AAs in the sample ($\delta^{13}C_{norAA} = \delta^{13}C_{AA}$ (of interest)-mean all AAs in sample) as described for the multivariate statistics required for the $\delta^{13}C$ fingerprinting approach described in Larsen et al. (2013). To assess if CSIA-AA can be used to separate bacterial isotopic values from sponge isotopic values, a principal component analysis (PCA) and linear discriminant analysis (LDA) were conducted on $\delta^{13}C_{norEAA}$ from the sponges at each depth using source end-member data from Larsen et al. (2013) and McMahon et al. (2016). It should be noted that the end-member source data used in these analyses while not depth-dependent, represent the best available data for invertebrates and their food sources, including representatives from coral reefs.

Differences in the mean of all $\delta^{13}C_{AA/EAA}$ and $\delta^{15}N_{AA/SAA/TAA}$, TP, and ΣV values between depths within each species were assessed using linear regression with depth as a continuous variable (significance level of $\alpha=0.05$). Differences in mean $\delta^{13}C_{AA/EAA}$ and $\delta^{15}N_{AA/SAA/TAA}$, TP and ΣV values between species were also assessed using analysis of variance (ANOVA) with Tukey HSD *post hoc* tests as needed (significance level of $\alpha=0.05$). Any data not meeting the assumptions of normality were log-transformed before analyses. The trophic position of sponges at each depth was calculated with $\delta^{15}N_{Phe}$ and $\delta^{15}N_{Glx}$ using a sponge species-specific enrichment factor calculated as described in Chikaraishi et al. (2014) using the formula:

$$TP_{Glx/Phe} = [(\delta^{15}N_{Glx} - \delta^{15}N_{Phe} + \beta)/TDF] + 1$$

where β represents the isotopic difference between $\delta^{15}N_{Glu}$ and $\delta^{15}N_{Phe}$ in aquatic cyanobacteria and algae (-3.4 ± 0.9‰). Species-specific discrimination factors (TDF) were calculated by subtracting the mean $\delta^{15}N_{SAA}$ from the mean $\delta^{15}N_{TAA}$ of each sponge, then the mean value of that calculation from each set of samples was calculated for use as the species-specific discrimination factor (*X. muta* = 8.077, *P. angulospiculatus* = 7.318, *A. tubulata* = 4.75). The ΣV value was calculated as outlined in McCarthy et al. (2007) and as described by Shih et al. (2020), using the average deviation of seven trophic $\delta^{15}N_{AA}$ values (Ala, Glu, Leu, Iso, Pro, Asx, Glx) for all samples as follows:

$$\Sigma V = 1/n \; \Sigma \; \text{Abs} \; (X_{AA})$$

Author Manuscript

where *X* of each trophic AA = ($\delta^{15}N_{AA}$ – AVG $\delta^{15}N_{AA}$ (Ala, Glu, Leu, Iso, Pro, Asx, Glx)), and *n* = the total number of $\delta^{15}N_{AA}$ used in the calculation.

Author Manuscript

Results

Sponge environment and survey results

From Morrow et al. (2016) vertical profiles of PAR for Little Cayman showed that the maximum surface irradiances were ~ 2400 µmol quanta m^{-2} s^{-1}. With a K_{dPAR} for the water column that ranged from 0.056 to 0.057 m^{-1}. Vertical profiles of temperature showed a well-mixed water column down to ~25 m at Little Cayman with surface temperature ~ 28.5°C at the surface and ~24.5°C at 91 m. For the percent cover of sponges with depth a significant increase was observed for *X. muta* ($t(28) = 8.60$, P = <0.0001), *A. tubulata* ($t(28) = 6.50$, P = <0.0001) and *P. angulospiculatus* ($t(28) = 8.61$, P = <0.0001) (Fig. 1) with the largest increase in percent cover coming at, or after, ~60 m depth for all species.

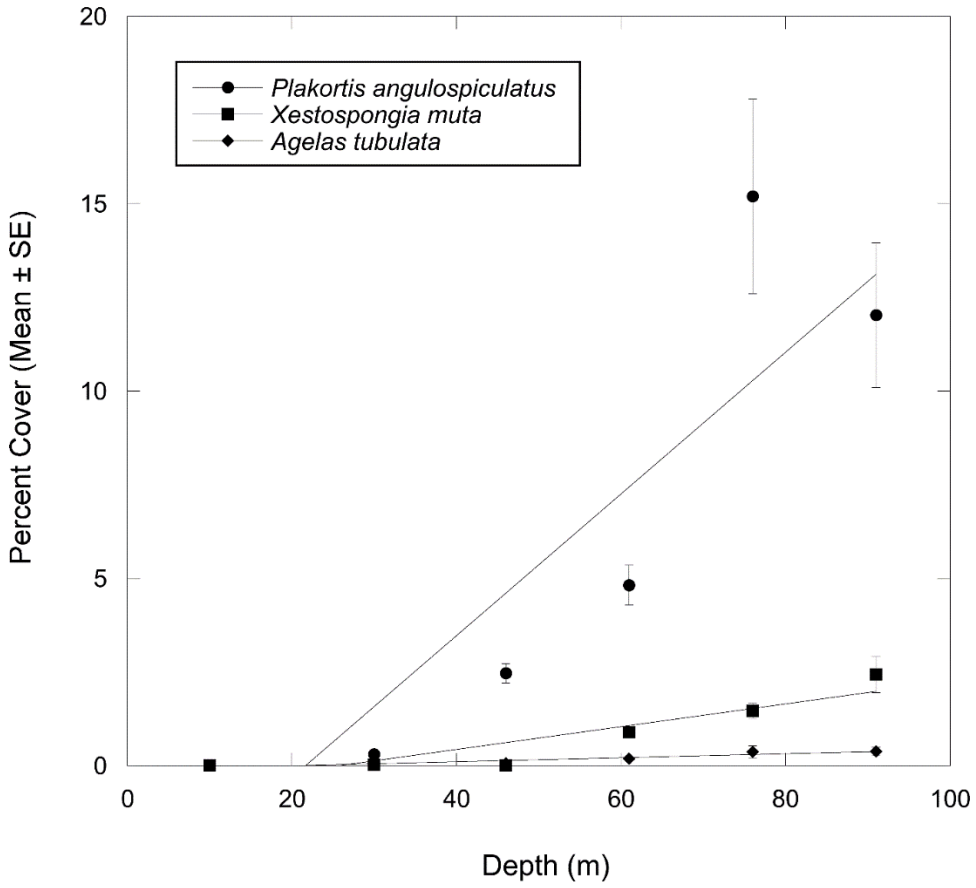

Figure 1. Percent cover per m^2 (mean ± SE) plot of sponges at 10, 18, 30, 61 and 91 m. Regression analysis for effect of depth were all significant: *Plakortis angulospeculatus*, y=-4.0968 + 0.18922x, R^2=0.787 (*t*(28) = 8.61, P = <0.0001), *Agelas tubulata*, y=-0.1105 + 0.0054x, R^2=0.893 (*t*(28) = 6.50, P = <0.0001), *Xestospongia muta*, y=-0.7867 + 0.0305x, R^2=0.831 (*t*(28) = 8.60, P = <0.0001).

Bulk stable isotope analyses:

The bulk stable isotopes of the three sponges show species-specific differences but all show a pattern of increasing values with increasing depth into the mesophotic zone (Fig. 2, Table 1). There were significant differences between all species in tissue $\delta^{13}C$ (ANOVA: F = 63.1331, P =

Author Manuscript

Author Manuscript

<0.0001, Tukey's HSD: P=<0.05), and $\delta^{15}N$ (ANOVA: F = 53.996P = <0.0001, Tukey's HSD: P=<0.05). There was also a significant effect observed, using regression analyses of the data in Table 1, of depth on the bulk tissue $\delta^{13}C$ (*t*(10) = 6.39, P = <0.0001) and $\delta^{15}N$ (*t*(10) = 3.07, P = 0.012) for *X. muta*, *A. tubulata* $\delta^{13}C$ (t(10) = 4.20, P = 0.001) and $\delta^{15}N$ (t(10) = 4.21, P = 0.001) and *P. angulospiculatus* $\delta^{13}C$ (*t*(10) = -3.01, P = 0.007) and $\delta^{15}N$ (*t*(10) = -260, P = 0.009).

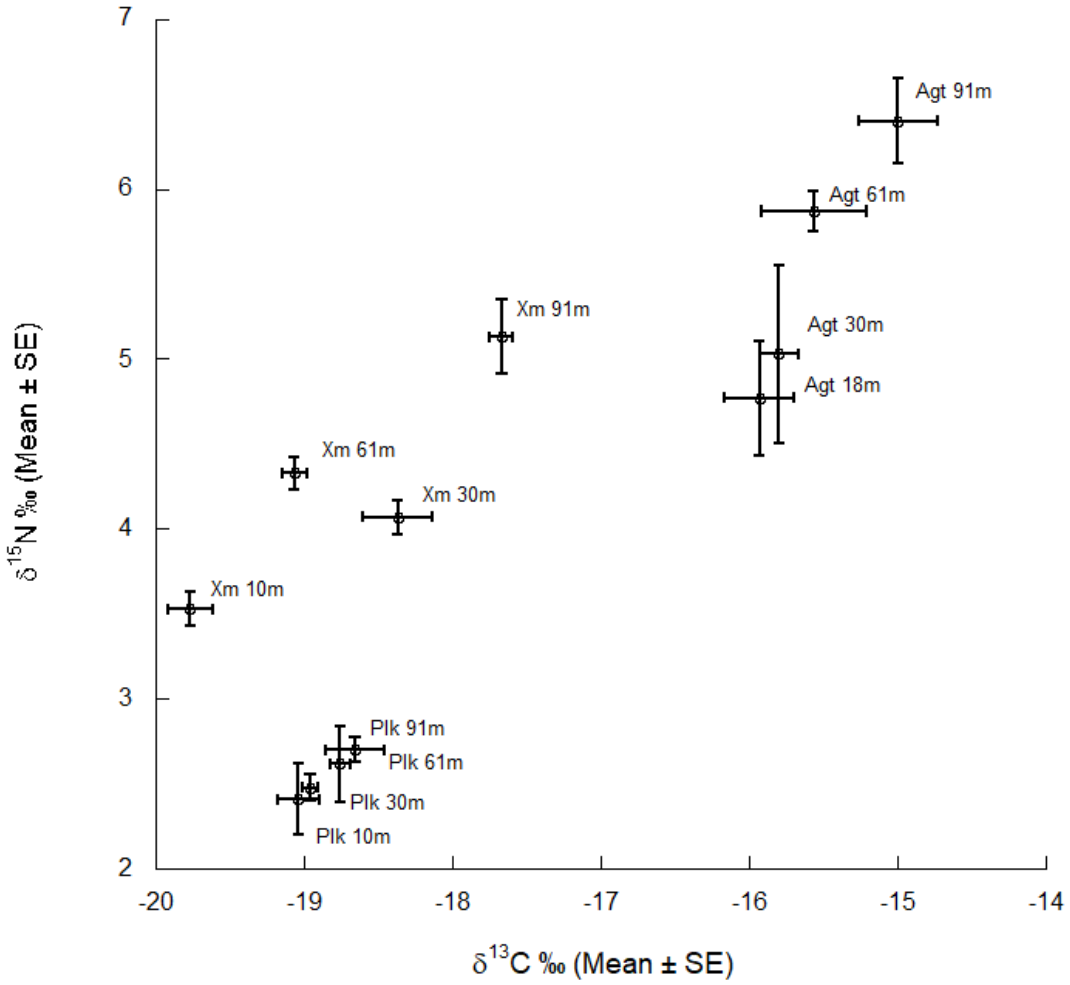

Figure 2. Bivariate plot of bulk stable isotope data for $\delta^{13}C$ and $\delta^{15}N$ from *Xestospongia muta* (Xm), *Plakortis angulospiculatus* (Plk) and *Agelas tubulata* (Agt).

Table 1. Means (±SE) of Bulk $\delta^{13}C$, Bulk $\delta^{15}N$, $\delta^{13}C_{EAA}$, $\delta^{15}N_{SAA,}$ $\delta^{15}N_{TAA,}$ trophic position (TP) and ΣV value data for the target species and all depths.

Species	Depth	Bulk $\delta^{13}C$ (± SE)	Bulk $\delta^{15}N$ (± SE)	$\delta13C_{EAA}$ (± SE)	$\delta15N_{SAA}$ (± SE)	$\delta15N_{TAA}$ (± SE)	TP phe-glu (± SE)	ΣV value (± SE)
X. muta	**10 m**	-19.77 (0.15)	3.53 (0.10)	-19.96 (0.53)	0.11 (0.21)	8.85(0.28)	2.03 (0.10)	1.65(0.04)
X. muta	**30 m**	-19.07 (0.08)	4.33 (0.09)	-19.41 (0.37)	-0.04 (0.44)	8.91 (0.95)	1.96 (0.19)	1.77 (0.01)
X. muta	**61 m**	-18.37 (0.23)	4.07 (0.10)	-19.73 (0.11)	0.74 (0.09)	8.79 (0.49)	1.85 (0.04)	1.43 (0.03)
X. muta	**91 m**	-17.67 (0.07)	5.13 (0.21)	-18.89 (0.33)	2.36 (0.29)	9.72 (0.21)	1.86 (0.05)	1.86 (0.01)
A. tubulata	**18 m**	-15.93 (0.23)	4.77 (0.33)	-19.48 (0.47)	1.40 (0.21)	5.96 (0.13)	1.74 (0.05)	0.85 (0.11)
A. tubulata	**30 m**	-15.80 (0.13)	5.03 (0.52)	-18.8 (0.25)	1.7 (0.28)	6.20 (0.35)	1.75 (0.10)	0.82 (0.11)
A. tubulata	**61 m**	-15.56 (0.35)	5.87 (0.12)	-18.92 (0.10)	2.175 (0.21)	6.89 (0.41)	1.90 (0.12)	0.98 (0.12)
A. tubulata	**91 m**	-15.00 (0.26)	6.40 (0.25)	-18.1 (1.16)	1.2 (0.57)	6.43 (0.31)	1.96 (0.19)	0.94 (0.08)
P. angulospiculatus	**10 m**	-19.04 (0.14)	2.41 (0.21)	-19.12 (0.21)	-1.23 (0.59)	5.61 (0.25)	1.66 (0.02)	1.47 (0.07)
P. angulospiculatus	**30 m**	-18.96 (0.05)	2.48 (0.08)	-19.75 (0.14)	0.133 (0.24)	6.69 (0.50)	1.56 (0.02)	1.5 (0.05)
P. angulospiculatus	**61 m**	-18.76 (0.06)	2.62 (0.22)	-18.83 (0.35)	-0.55 (0.33)	6.98 (0.16)	1.40 (0.23)	1.48 (0.08)
P. angulospiculatus	**91 m**	-18.66 (0.19)	2.70 (0.07)	-17.71 (0.16)	-0.175 (0.44)	8.15 (0.08)	1.63 (0.23)	1.79 (0.09)

Compound specific isotope analyses of amino acids

The $\delta^{13}C_{EAA}$ fingerprinting analysis, using the Larsen et al. (2013) $\delta^{13}C_{EAA}$ training data set, showed that sponges' group separately from most other organisms, but by sponge species (Fig. 3). In both analyses, sponges with known symbionts are differentiated from their potential food sources such as microalgae, fungus, and bacteria, with microalgae grouping closely with macroalgae. The LDA was used to assess biosynthetic origin of sponge carbon, and the LDA predicted potential end-member groups with 91% accuracy. All sponges are primarily classified

Author Manuscript

with bacteria, detritus, microalgae or macroalgae but not POM (plankton collection using 5 μm mesh net) (Fig. 4).

To quantify changes in trophic strategy between depths, an ANOVA was used on species and linear regression was applied to the mean values of all $\delta^{13}C_{EAA}$, $\delta^{15}N_{SAA,}$ $\delta^{15}N_{TAA,}$ TP and ΣV measurements between depths for each species (Table 1, Fig. 5). There were no significant differences in $\delta^{13}C_{EAA}$ between species (ANOVA: F = 2.2217, P = 0.124). There were significant differences in $\delta^{15}N_{SAA}$ (ANOVA: F = 17.1226, P = <0.0001), with *P. angulospiculatus* significantly lower than both *X. muta* and *A. tubulata* (Tukey's HSD: P<0.05), and significant differences in $\delta^{15}N_{TAA}$ (ANOVA: F = 32.403, P = <0.0001), with *X. muta* significantly greater than *P. angulospiculatus* and *A. tubulata* (Tukey's HSD: P=<0.05). Significant differences were detected (ANOVA: F = 11.432, P = 0.0002) in TP between species with *P. angulospiculatus* significantly lower than *A. tubulata* and *X. muta* (Tukey's HSD: P=<0.05). There were significant differences between species for ΣV values, with higher values indicating more microbial repossessing and translocation of organic matter to the host (ANOVA: F = 69.702, P = <0.0001). *Post-hoc* comparisons revealed that *A. tubulata* was significantly lower than *X. muta* and *P. angulospiculatus* (Tukeys HSD: P=<0.05) (Table 1).

Using regression analysis there was no significant effect of depth on $\delta^{13}C_{EAA}$ ($t(10) = 1.73$, P = 0.114), $\delta^{15}N_{TAA}$ ($t(10) = 1.08$, P = 0.305), TP ($t(10) = -1.29$, P = 0.225) or ΣV value ($t(10) =$ 0.63, P = 0.541) for *X. muta*, (Table 1). But there was a significant effect of depth on $\delta^{15}N_{SAA}$ ($t(10) = 4.97$, P = <0.0001) (Table 1). For *A. tubulata* there was no significant effect of depth on $\delta^{13}C_{EAA}$ ($t(10) = 1.51$, P = 0.163), $\delta^{15}N_{SAA}$ (t(10) = -0.18, P = 0.864), $\delta^{15}N_{TAA}$ (t(10) = 1.38, P = 0.197), TP ($t(10) = 1.61$, P = 0.138) or ΣV value ($t(10) = 0.99$, P = 0.3471) (Table 1). For *P. angulospiculatus* there was no significant effect of depth on $\delta^{15}N_{SAA}$ ($t(10) = 1.02$, P = 0.332) or

Author Manuscript

TP ($t(10) = -0.41$, P = 0.689), while there was a significant effect of depth on $\delta^{13}C_{EAA}$ ($t(10) = 3.71$, P = 0.004), $\delta^{15}N_{TAA}$ ($t(10) = 5.78$, P = 0.001), and ΣV value ($t(10) = 2.55$, P = 0.0287) (Table 1).

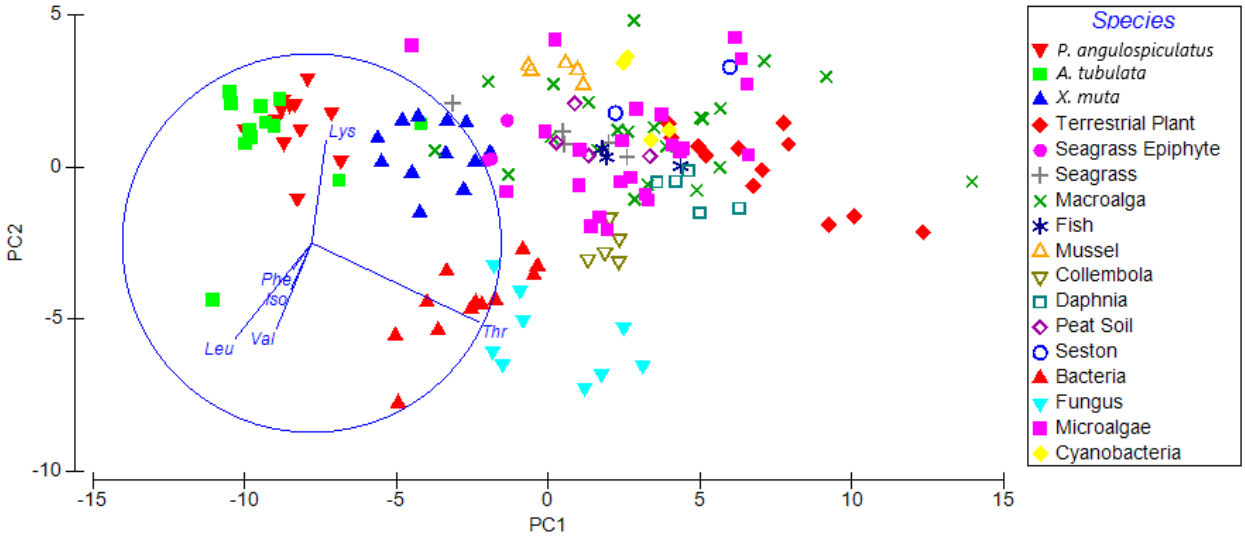

Figure 3. Fingerprinting method for separating functional groups based on principal component analysis of CSIA $\delta^{13}C_{norEAA}$ data. Sponge $\delta^{13}C_{norEAA}$ values are unique, species-specific and well separated compared to potential food resources of prokaryotic and eukaryotic origin, as well as other filter feeding organisms (e.g. mussels) taken from Larsen et al. (2013).

Author Manuscript

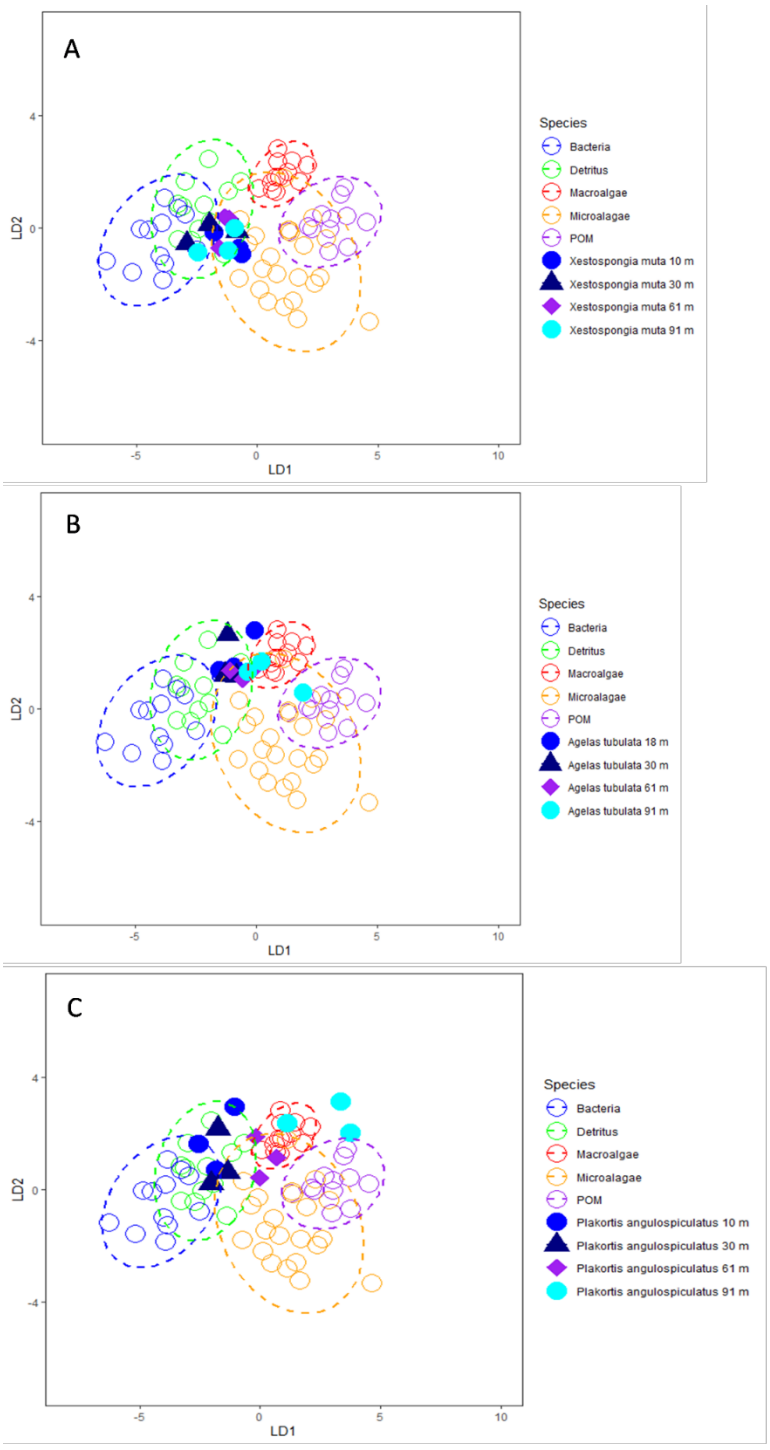

Figure 4. Linear discriminant analysis plots from CSIA $\delta^{13}C_{norEAA}$ data from A) *Agelas tubulata* B) *X. muta* and C) *P. angulospiculatus.* Source end-member data was taken from the Larsen et al. (2013) CSIA $\delta^{13}C_{norEAA}$ and from McMahon et al. (2016).

Author Manuscript

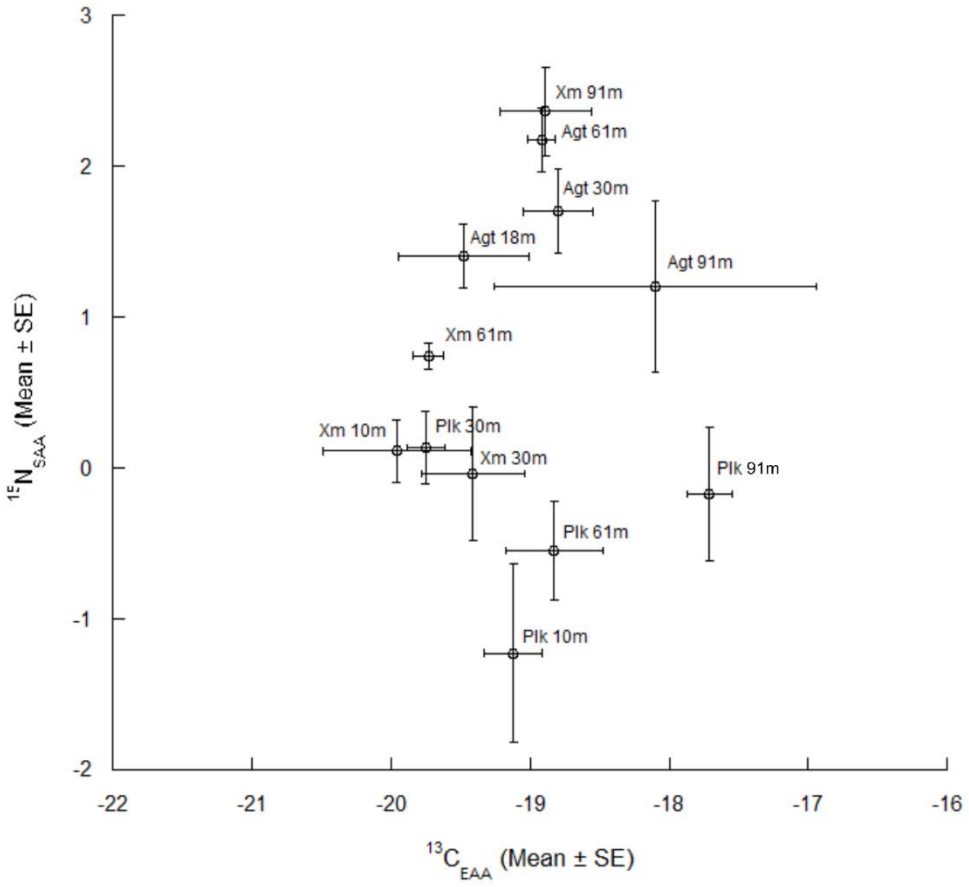

Figure 5. Bivariate plot of mean CSIA $\delta^{13}C_{EAA}$ and $\delta^{15}N_{SAA}$ stable isotope data from *Xestospongia muta* (Xm), *Plakortis angulospiculatus* (Plk) and *Agelas tubulata* (Agt).

Discussion

The sponge species used for this study show an increase in percent cover from shallow to mesophotic depths in Little Cayman consistent with sponges from multiple locations in the Caribbean (Lesser & Slattery 2018), and the Pacific (Slattery & Lesser 2012, Lesser & Slattery 2018). The increase in sponge cover also occurs at the beginning of the lower mesophotic (~60 m) and is consistent with recent observations of global faunal breaks for mesophotic taxa on coral reefs (Lesser et al. 2019). Sponge cover increases with depth (Fig. 1), and are known to

Author Manuscript

Author Manuscript

grow faster and have increased scope for growth as depth increases in the Caribbean at both shallow and mesophotic depths (Trussell et al. 2006, Lesser 2006, Lesser & Slattery, 2018). Previous studies have shown this pattern to be associated with increased particulate trophic resources available to them as depth increases (Lesser 2006, Slattery & Lesser 2011, Lesser et al. 2019, 2020). Specifically, particulate nitrogen availability increases with depth (Lesser et al. 2019, 2020) and may play a key role in the patterns of sponge distribution in the Caribbean mesophotic zone (de Geoij et al. 2017).

The bulk SIA data from the three sponges in this study shows a species-specific pattern as depth increases (Fig. 2). The $\delta^{13}C$ values reflect the consumption of both photoautotrophically produced DOM and photoautotrophic and heterotrophic POM (Table 1, $\delta^{13}C$ marine picoplankton: -19 to -24‰, DOM: -16 to -23‰) (Fry 2006, Slattery & Lesser 2011, Hansell 2014, van Duyl et al. 2011, 2018), as well as fractionation processes, such as carbon or nitrogen cycling, and photoautotrophy, facilitated by the species-specific microbiomes of these sponges. The data show that heterotrophy increases with increasing depth as lighter isotopes are favored during waste excretion leading to an increase in $\delta^{15}N$ values at higher trophic levels (i.e. more of the heavier isotope leads to an increase in $\delta^{15}N$ values). The increases in both $\delta^{13}C$ and $\delta^{15}N$ suggest an increased, and proportional, reliance on heterotrophic picoplankton as photoautotrophic picoplankton declines into the mesophotic zone as reported previously (Lesser 2006, Trussell et al. 2006, Slattery & Lesser 2011).

Analyses of the CSIA-AA data, using the $\delta^{13}C_{norEAA}$ fingerprinting method based on the Larsen et al. (2013) training dataset and data from McMahon et al. (2016), reveals that sponge $\delta^{13}C_{norEAA}$ values are both unique to sponges and species-specific when compared to the $\delta^{13}C_{norEAA}$ of a wide range of both prokaryotic and eukaryotic organisms (Fig 3). Sponges were

Author Manuscript

unambiguously separated from their principal planktonic food sources such as cyanobacteria and free-living bacteria (Fig. 3). This was possible despite the fact that sponges host a microbiome consisting of these groups in their tissues. This suggests fundamental differences in the microbial communities of sponges versus the bacterioplankton of the surrounding seawater that can be distinguished using CSIA-AA. For instance, there are multiple aerobic or anaerobic microenvironments within a sponge (Fiore et al. 2010) that are linked to the metabolic diversity found in sponge microbiomes (Hentschel et al. 2012, Fiore et al. 2015, Pita et al. 2018) a wide range of $\delta^{13}C_{norEAA}$ values from these metabolic pathways could be contributing to the observed ability to discriminate between the sponge microbiome and the ambient bacterioplankton communities.

An LDA (Fig. 4) of $\delta^{13}C_{norEAA}$ was used to assess the source end-member each sponge sample classified most closely with, based on data from Larsen et al. (2013) and McMahon et al. (2016). All sponges classify most closely with bacteria, detritus and macroalgae (a proxy for DOM), suggesting a reliance on a mixed diet of POM and DOM at all depths. The LDA also reveals patterns which are likely a result of the species-specific microbiomes utilization of DOM and in the case of *X. muta*, a loss of cyanobacterial photosynthate due to reductions in available PAR, or reductions in cyanobacterial symbiont abundances with depth (Morrow et al. 2016). This is also seen in the significant increases in the bulk $\delta^{13}C$ and the trend of increases in the $\delta^{13}C_{EAA}$, the indicating potential reductions in carbon fixed via photoautotrophy as depth increases. The DOM consumed by sponges could be used for microbial production of essential amino acids, as essential amino acids are derived from microbial, algal or plant organic material and cannot be synthesized *de novo* in animals (Larsen et al. 2009, 2013, McMahon et al. 2016). The microbiome may then translocate (*sensu* Fiore et al. 2015, Shih et al. 2020) specific nutrients

Author Manuscript

to the host or be consumed directly through phagocytosis (*sensu* Leys et al. 2018) to be used for sponge growth. It is evident that DOM is an important component of the diets of the sponge holobiont but as the LDA classifies the most likely source for each sponge sample, it may not detect finer scale patterns such as changes in the quantity of particular source-end member (i.e. an increase in lower C:N ratio bacterioplankton available as depth increases).

To examine fine scale changes in diet, the mean $\delta^{13}C_{EAA}$, $\delta^{15}N_{SAA,}$ $\delta^{15}N_{TAA,}$ ΣV and TP values between depths for each species have the potential to be informative as it relates to the diet of these sponges and the metabolic processes of host and its microbiome at each depth (McCarthy et al. 2007, Larsen et al. 2013, Vokshoori et al. 2014, McMahon et al. 2016). The mean $\delta^{13}C_{EAA}$ of these sponges reflect a diet of both picoplankton and DOM (Fig. 5), but the species-specific patterns observed in the bulk data (Fig. 2) were not observed. This suggests that selective feeding is not occurring here, but instead non-selective filtering and utilization of both DOM and POM resources, based on their availability, occurs at all depths. Since resource availability changes with depth, such as the increase in heterotrophic picoplankton and reduced input from photoautotrophy in the mesophotic zone (Lesser 2006, Lesser et al. 2018, 2020), it is highly probable that the patterns of increases in mesophotic sponge $\delta^{13}C_{EAA}$ are driven by the change in resource availability. The increases in $\delta^{13}C_{EAA}$ do not appear to be driven by depth related changes in the microbial community structure of these sponges, as *A. tubulata* shows no significant change in microbiome community structure along the depth gradient (Olson & Gao 2013, Macartney & Lesser, unpublished). The $\delta^{13}C_{EAA}$, however, does follow a similar pattern with depth in *X. muta* and *P. angulospiculatus* where significant changes in their microbiome communities from shallow to mesophotic depths were observed (Olson & Gao 2013, Morrow et al. 2016, Macartney & Lesser, unpublished). Given that sponge species that do, and do not,

Author Manuscript

exhibit changes in their microbiome communities still show a pattern of increases in $\delta^{13}C_{EAA}$ with depth, a functional analysis (i.e., isotope tracer studies) would be needed to fully resolve the role of the microbiome on $\delta^{13}C_{EAA}$ values. Recently, however, Shih et al. (2020) showed that the $\delta^{13}C_{EAA}$ and $\delta^{15}N_{SAA}$ of host and symbiont cells in the sponge, *Mycale grandis* are not significantly different, and that their high ΣV values, a measure of bacterial re-synthesis and translocation of organic material (i.e., amino acids), indicated that these sponges obtained a significant amount of their nutrition directly from their symbionts.

All three of the sponge species examined show low $\delta^{15}N_{SAA}$ values suggesting that all sponges are consuming resources produced by diazotrophs during nitrogen fixation (-2 to 2‰) (Fig. 5, Table 1, Table S2). However, the potential for nitrogen fixation has been previously reported in sponges (Mohammed et al. 2008, Fiore et al. 2013), and sponge tissues appear well oxygenated during pumping (Schlappy et al. 2010, Fiore et al. 2013, Leys et al. 2018) which would normally inhibit nitrogen fixation as the enzyme nitrogenase is sensitive to oxygen (Fiore et al. 2010). A more parsimonious explanation for the low values would be consumption of isotopically light picoplankton and DOM, which are present at all depths, but decrease in abundance with depth (Lesser 2006). Sponges can also consume unicellular picoplankton such as *Crocosphaera* sp. and *Cyanothece* sp. that fix nitrogen (Bauercachs et al. 2009), which would also contribute to the depleted value observed here. Populations of unicellular cyanobacteria decrease, while *Prochlorococcus* and heterotrophic picoplankton increase into the mesophotic (Lesser 2006, Lesser et al. 2020). *Prochlorococcus*, and most marine species of *Synechoccocus*, are not known to fix nitrogen and their $\delta^{15}N$ value likely reflects the $\delta^{15}N$ isotopic values of DIN in the water column (~3 to 6‰) (Slattery & Lesser 2011, Ren et al. 2012) so the increased consumption of both heterotrophic bacteria and *Prochlorococcus* is likely contributing to the

observed pattern of $\delta^{15}N$ increases as depth increases in *P. angulospiculatus* and *X. muta*. However, anoxic compartments do occur in sponge tissues, so a combined effect of microbiome-associated nitrogen fixation and feeding on isotopically lighter picoplankton cannot be ruled out.

Interestingly, the $\delta^{15}N_{SAA}$ of *P. angulospiculatus* and *A. tubulata* do not undergo significant increases with depth indicating that increases in the bulk $\delta^{15}N$ may be a result of microbial transformations of other macromolecules (i.e. fatty acids of lipids) or changes in trophic resources stable isotope composition instead of increased consumption of heterotrophic bacteria. This is contrary to multiple feeding studies (Lesser 2006, Trussell 2006), but it is clear that POM as a resource increases with depth (Lesser 2006, Trussell et al. 2006, Lesser et al. 2019), so while the CSIA-AA signatures of sponges may not reflect a change in diet type, they are still likely feeding proportionately on the increased quantities of POM as depth increases (Morganti et al. 2017). Additionally, the $\delta^{15}N_{SAA}$ of *A. tubulata* were higher relative to the other sponges in this study, indicating that this sponge relies more heavily on heterotrophy at all depths studied. The observed $\delta^{15}N_{TAA}$ values from all sponges show increases consistent with one trophic level of fractionation (Hannides et al. 2009, Chickariashi et al. 2009, 2014), confirming that sponges consume both picoplankton and DOM. The increased values of $\delta^{15}N_{TAA}$ values along the depth gradient observed in *P. angulospiculatus* and *X. muta* (Table 1) also indicate that there is increased trophic enrichment as depth increases (i.e., consumption of POM), and a decrease in the consumption of photoautotrophically derived resources. In the case of *X. muta*, the significant increase in $\delta^{15}N_{SAA}$ is also driven by increased heterotrophy over autotrophy as depth increases. The lack of any significant changes $\delta^{15}N_{TAA}$ in *A. tubulata* appears to indicate that it relies on a similar trophic strategy along the depth gradient and any trophic inputs from the microbiome remain stable as does the observed ΣV value of this sponge.

Author Manuscript

Author Manuscript

The ΣV value of a sponge sample can be used as a proxy for the microbial resynthesis of amino acids within the sponge (McCarthy et al. 2007, Shih et al. 2020). The microbiomes of sponges and sponge cells are known to consume DOM as it is pumped through the host sponge (Rix et al. 2016). The byproducts of metabolizing DOM or photosynthesis by the microbiome are known to be translocated to host cells or through direct symbiont consumption via phagocytosis in the mesohyl (Fiore et al. 2015, Leys et al. 2018, Pita et al. 2018). The ΣV values for all sponges in this study are below 2 which is similar to values seen in zooplankton (McCarthy et al. 2007, Shih et al. 2020) (Table 1). This indicates that while DOM re-synthesis by the microbiome and subsequent transfer to the host is occurring in these sponges, the sponge host is still obtaining food from heterotrophic feeding on picoplankton.

The higher ΣV values in *X. muta* and *P. angulospiculatus* compared to *A. tubulata* (Table 1) suggests that *X. muta* and *P. angulispiculatus* rely more on microbial reprocessing of DOM at all depths. In particular, the significant increase in *P. angulospiculatus* ΣV values with depth suggests that this sponge relies more on their microbial symbionts with depth for DOM consumption and reprocessing relative to shallow conspecifics and may be more dependent on DOM compared to the other sponges in this study. This also appears to be reflected in its TP values which are lower compared to the other sponges. Additionally, their microbiomes may play a larger role in processing waste products that the sponge produces from heterotrophic feeding, such as ammonia. Many sponges are known to have ammonia oxidizing bacteria present in their mesohyl and genomic evidence shows waste uptake in several common sponge symbionts (Hentschel et al. 2012, Pita et al. 2018). The lower ΣV value of *A. tubulata* corroborates the observed reliance on heterotrophy at all depths in this sponge based on its $\delta^{15}N_{SAA}$. Interestingly these sponges show lower ΣV values compared the encrusting sponge

Author Manuscript

Mycale grandis (ΣV value: 3) (Shih et al. 2020), which suggests that emergent sponges rely less on DOM compared to encrusting sponges. This has been suggested previously, as encrusting sponges are better suited for DOM uptake in terms of total surface area (de Goeij et al. 2017). While this study did not separate microbial symbionts from sponge tissues, data from Shih et al. (2020) showed no significant difference in CSIA-AA isotopic composition between sponge tissues and its microbiome.

The TP values of the sponges' in this study range between 1-2 (Table 1), indicating that they are primary consumers on Caribbean coral reefs (Hannides et al. 2009, Mompean et al. 2015, Landry et al. 2017) that utilize both POM and DOM. The differences between species may indicate that there are different strategies in microbiome assimilation of DOM or species specific differences reliance of the host on the microbiome for nutrition. The ΣV and TP values together provide evidence of consumption of POM and DOM by the sponges in this study at all depths, but increased POM consumption as depth increases consistent with the observed patterns of increases in the picoplankton fraction of POM in the mesophotic throughout the Caribbean (Lesser 2006, Lesser et al. 2019, 2020). We also show that the microbiomes of sponges provide species specific nutritional inputs to their hosts. However, given the variability between the three HMA sponges described here we suggest that the trophic ecology of sponges should be assessed on a species by species basis.

Conclusions

Based on the bulk SIA data from this study, mesophotic sponges have increased reliance on POM consumption based on the pattern of increasing of $\delta^{13}C$ and $\delta^{15}N$. However, these patterns also suggest that these sponges may have varying trophic strategies (i.e. feeding on different end-

members) or have species-specific transformations of carbon and nitrogen due to their unique microbiomes. The CSIA-AA data shows that these sponges feed in the same trophic niche at each depth, consuming DOM and POM in proportion to its availability at all depths but with varying contributions of nutrition from their microbiomes through microbial reprocessing of DOM based on ΣV values. Consumption of DOM is crucial for sponge nutrition but increased quantities of POM as depth increases appears to support the co-occurring increase in sponge biomass. While the increases in mean $\delta^{13}C_{EAA}$ and $\delta^{15}N_{SAA}$ are lower compared to bulk data as depth increases, this is to be expected due to the lack of fractionation processes (Larsen et al. 2009, 2013). The ΣV values from these sponges show that these sponges utilize resynthesized amino acids from their microbiome to varying degrees but also that these sponges rely on both DOM and POM for their carbon and nitrogen budgets at all depths assessed here. This study provides comprehensive evidence that CSIA-AA has the potential to increase our understanding of Caribbean mesophotic coral reef trophic ecology and sets a baseline that can be expanded upon with additional studies of sponge microbiome community structure, increased source-end member sampling for multivariate analyses, and *in-situ* feeding measurements of sponges in the mesophotic zone.

Acknowledgements

We thank K. Morrow, E. Kintzing, C. Fiore, D. Gochfeld and J. Jarett for field and laboratory support. We thank S. Pankey for comments on sponge microbiomes and statistical analysis. We thank Dr. Brian Popp and Natalie Wallsgrove at the University of Hawaii Biogeochemical Stable Isotope Facility for conducting the CSIA of Amino Acids. All sample collections complied with the laws of the Cayman Islands and the United States of America. This project was funded by the

Author Manuscript

National Science Foundation, Biological Oceanography (OCE–1632348/1632333) to MPL and MS and NOAA NIUST (14U752) to MS and MPL. The authors declare no competing conflicts of interest.

Author Manuscript

Author Manuscript

Literature Cited

Bauersachs T, Schouten S, Compaoré J, Wollenzien U, Stal LJ, Damsteé JSS (2009) Nitrogen isotopic fractionation associated with growth on dinitrogen gas and nitrate by cyanobacteria. Limnol Oceanogr 54:1403–1411.

Bell JJ (2008) The functional roles of marine sponges. Estuar Coast Shelf Sci 79:341–353.

Bell JJ, Davy SK, Jones T, Taylor MW, Webster NS (2013) Could some coral reefs become sponge reefs as our climate changes? Glob Chang Biol 19:2613–2624.

Bell JJ, Rovellini A, Davy SK, Taylor MW, Fulton EA, Dunn MR, Bennett HM, Kandler NM, Luter HM, Webster NS (2018) Climate change alterations to ecosystem dominance: how might sponge-dominated reefs function? Ecology 99:1920–1931.

Chikaraishi Y, Ogawa NO, Kashiyama Y, Takano Y, Suga H, Tomitani A, Miyashita H, Kitazato H, Ohkouchi N (2009) Determination of aquatic food-web structure based on compound-specific nitrogen isotopic composition of amino acids. Limnol Oceanogr Methods 7:740–750.

Chikaraishi Y, Steffan SA, Ogawa NO, Ishikawa NF, Sasaki Y, Tsuchiya M, Ohkouchi N (2014) High-resolution food webs based on nitrogen isotopic composition of amino acids. Ecol Evol 4:2423–2449.

Diaz MC, Rützler K (2001) Sponges: an essential component of Caribbean coral reefs. Bulletin of Marine Science, 69: 535-546.

van Duyl FC, Moodley L, Nieuwland G, van Ijzerloo L, van Soest RWM, Houtekamer M, Meesters EH, Middelburg JJ (2011) Coral cavity sponges depend on reef-derived food resources: stable isotope and fatty acid constraints. Mar Biol 158:1653–1666.

van Duyl FC, Mueller B, Meesters EH (2018) Spatiotemporal variation in stable isotope signatures (13C and 15N) of sponges on the Saba Bank. PeerJ 6:e5460.

Fiore CL, Baker DM, Lesser MP (2013) Nitrogen Biogeochemistry in the Caribbean Sponge, *Xestospongia muta*: A Source or Sink of Dissolved Inorganic Nitrogen? PLoS One 8:e72961.

Fiore CL, Jarett JK, Olson ND, Lesser MP (2010) Nitrogen fixation and nitrogen transformations in marine symbioses. Trends Microbiol 18:455–463.

Fiore CL, Labrie M, Jarett JK, Lesser MP (2015) Transcriptional activity of the giant barrel sponge, *Xestospongia muta* holobiont: molecular evidence for metabolic interchange. Front Microbiol 6:364.

Fry B (2006) Using Stable Isotope Tracers. In: *Stable Isotope Ecology*. Springer New York, p 40–75

Gili J-M, Coma R (1998) Benthic suspension feeders: their paramount role in littoral marine food webs. Trends Ecol Evol 13:316–321.

Gloeckner V, Wehrl M, Moitinho-Silva L, Gernert C, Schupp P, Pawlik JR, Lindquist NL, Erpenbeck D, Wörheide G, Hentschell U (2014) The HMA-LMA dichotomy revisited: an electronmicroscopical survey of 56 sponge species. Bio Bull 227:78-88.

de Goeij JM, Lesser MP, Pawlik JR (2017) Nutrient Fluxes and Ecological Functions of Coral Reef Sponges in a Changing Ocean. In: *Climate Change, Ocean Acidification and Sponges*. Springer International Publishing, p 373–410

Author Manuscript

de Goeij JM, van Oevelen D, Vermeij MJA, Osinga R, Middelburg JJ, de Goeij AFPM, Admiraal W (2013) Surviving in a marine desert: the sponge loop retains resources within coral reefs. Science (80-) 342:108–110.

Hadas E, Shpigel M, Ilan M (2009) Particulate organic matter as a food source for a coral reef sponge. J Exp Biol 212:3643–3650.

Hannides CCS, Popp BN, Landry MR, Graham BS (2009) Quantification of zooplankton trophic position in the North Pacific Subtropical Gyre using stable nitrogen isotopes. Limnol Oceanogr 54:50–61.

Hansell DA and Carlson CA (2014). *Biogeochemistry of marine dissolved organic matter*. Academic Press.

Hentschel U, Piel J, Degnan SM, Taylor MW (2012) Genomic insights into the marine sponge microbiome. Nat Rev Microbiol 10:641–654.

Hoegh-Guldberg O, Mumby PJ, Hooten AJ, Steneck RS, Greenfield P, Gomez E, Harvell CD, Sale PF, Edwards AJ, Caldeira K, Knowlton N, Eakin CM, Iglesias-Prieto R, Muthiga N, Bradbury RH, Dubi A, Hatziolos ME (2007) Coral reefs under rapid climate change and ocean acidification. Science 318:1737–1742.

Hughes TP, Barnes ML, Bellwood DR, Cinner JE, Cumming GS, Jackson JBC, Kleypas J, van de Leemput IA, Lough JM, Morrison TH, Palumbi SR, van Nes EH, Scheffer M (2017) Coral reefs in the Anthropocene. Nature 546:82–90.

Hughes TP, Kerry JT, Baird AH, Connolly SR, Dietzel A, Eakin CM, Heron SF, Hoey AS, Hoogenboom MO, Liu G, McWilliam MJ, Pears RJ, Pratchett MS, Skirving WJ, Stella JS, Torda G (2018) Global warming transforms coral reef assemblages. Nature 556:492–496.

Author Manuscript

Landry MR, Décima MR (2017) Protistan microzooplankton and the trophic position of tuna: quantifying the trophic link between micro- and mesozooplankton in marine foodwebs. ICES J Mar Sci 74:1885–1892.

Larsen T, Taylor DL, Leigh MB, OBrien DM (2009) Stable isotope fingerprinting: a novel method for identifying plant, fungal, or bacterial origins of amino acids. Ecology 90:3526–3535.

Larsen T, Ventura M, Andersen N, O'Brien DM, Piatkowski U, McCarthy MD (2013) Tracing Carbon Sources through Aquatic and Terrestrial Food Webs Using Amino Acid Stable Isotope Fingerprinting. PLoS One 8:e73441.

Lesser MP (2006) Benthic-pelagic coupling on coral reefs: Feeding and growth of Caribbean sponges. J Exp Mar Bio Ecol 328:277–288.

Lesser MP, Slattery M (2013) Ecology of Caribbean Sponges: Are Top-Down or Bottom-Up Processes More Important? PLoS One 8:e79799.

Lesser MP, Slattery M (2018) Sponge density increases with depth throughout the Caribbean. Ecosphere 9:e02525.

Lesser MP, Slattery M, Laverick JH, Macartney KJ, Bridge TC (2019) Global community breaks at 60 m on mesophotic coral reefs. Glob Ecol Biogeogr 28:1403–1416.

Lesser MP, Slattery M, Leichter JJ (2009) Ecology of mesophotic coral reefs. J Exp Mar Bio Ecol 375:1–8.

Lesser MP, Slattery M, Mobley CD (2018) Biodiversity and functional ecology of mesophotic coral reefs. Ann Rev Ecol Evol Syst 49:49–71.

Author Manuscript

Lesser MP, Mueller B, Pankey MS, Macartney KJ, Slattery M, de Goeij JM (2020) Depth-dependent detritus production in the sponge, *Halisarca caerulea*. Limnol Oceaogr doi: 10.1002/lno.11384.

Leys SP, Kahn AS, Fang JKH, Kutti T, Bannister RJ (2018) Phagocytosis of microbial symbionts balances the carbon and nitrogen budget for the deep-water boreal sponge *Geodia barretti*. Limnol Oceanogr 63:187-202.

Loya Y, Eyal G, Treibitz T, Lesser MP, Appeldoorn R (2016) Theme section on mesophotic coral ecosystems: advances in knowledge and future perspectives. Coral Reefs 35:1–9.

Maldonado M, Ribes M, van Duyl FC (2012) Nutrient fluxes through sponges: biology, budgets, and ecological implications. Adv Mar Biol 62:113–182.

McCarthy MD, Benner R, Lee C, Fogel ML (2007) Amino acid nitrogen isotopic fractionation patterns as indicators of heterotrophy in plankton, particulate, and dissolved organic matter. Geochim Cosmochim Acta 71:4727–4744.

McClelland JW, Montoya JP (2002) Trophic relationships and the nitrogen isotopic composition of amino acids in plankton. Ecology 83:2173-2180.

McMahon KW, Polito MJ, Abel S, McCarthy MD, Thorrold SR (2015) Carbon and nitrogen isotope fractionation of amino acids in an avian marine predator, the gentoo penguin (*Pygoscelis papua*). Ecol Evol 5:1278–1290.

McMahon KW, Thorrold SR, Houghton LA, Berumen ML (2016) Tracing carbon flow through coral reef food webs using a compound-specific stable isotope approach. Oecologia 180:809–821.

Author Manuscript

McManus J (2000) Coral reef fishing and coral-algal phase shifts: implications for global reef status. ICES J Mar Sci 57:572–578.

McMurray SE, Henkel TP, Pawlik JR (2010) Demographics of increasing populations of the giant barrel sponge *Xestospongia muta* in the Florida Keys. Ecology 91:560–570.

Mompeán C, Bode A, Gier E, McCarthy MD (2016) Bulk vs. amino acid stable N isotope estimations of metabolic status and contributions of nitrogen fixation to size-fractionated zooplankton biomass in the subtropical N Atlantic. Deep Sea Res I Oceanogr Res Pap 114:137–148.

Morrow KM, Fiore CL, Lesser MP (2016) Environmental drivers of microbial community shifts in the giant barrel sponge, *Xestospongia muta*, over a shallow to mesophotic depth gradient. Environ Microbiol 18:2025–2038.

Mueller B, de Goeij JM, Vermeij MJA, Mulders Y, van der Ent E, Ribes M, van Duyl FC (2014) Natural diet of coral-excavating sponges consists mainly of dissolved organic carbon (DOC). PLoS One 9:e90152.

Olson JB, Gao X (2013) Characterizing the bacterial associates of three Caribbean sponges along a gradient from shallow to mesophotic depths. FEMS Microbiol Ecol 85:74–84.

Pile AJ, Patterson MR, Savarese M, Chernykh VI, Fialkov VA (1997) Trophic effects of sponge feeding within Lake Baikal's littoral zone. 2. Sponge abundance, diet, feeding efficiency, and carbon flux. Limnol Oceanogr 42:178-184

Pita L, Rix L, Slaby BM, Franke A, Hentschel U (2018) The sponge holobiont in a changing ocean: from microbes to ecosystems. Microbiome 6:46.

Author Manuscript

Ren H, Sigman DM, Thunell RC, Prokopenko MG (2012) Nitrogen isotopic composition of planktonic foraminifera from the modern ocean and recent sediments. Limnol Oceanogr 57:1011–1024.

Rix L, de Goeij JM, Mueller CE, Struck U, Middelburg JJ, van Duyl FC, Al-Horani FA, Wild C, Naumann MS, van Oevelen D (2016) Coral mucus fuels the sponge loop in warm- and cold-water coral reef ecosystems. Sci Rep 6.

Shih JL, Selph KE, Wall CB, Wallsgrove NJ, Lesser MP, Popp BN (2020) Trophic tcology of the Tropical Pacific sponge *Mycale grandis* inferred from amino acid compound-specific isotopic analyses. Microb Ecol 79:495-510.

Slattery M, Lesser MP, Brazeau D, Stokes MD, Leichter JJ (2011) Connectivity and stability of mesophotic coral reefs. J Exp Mar Bio Ecol 408:32–41.

Slattery M, & Lesser MP (2012). Mesophotic coral reefs: a global model of community structure and function. Proc 12th Intl Coral Reef Symp 1:9-13.

Slattery M, Lesser M P (2015) Trophic ecology of sponges from shallow to mesophotic depths (3 to 150 m): Comment on Pawlik et al. (2015) . Mar Ecol Prog Ser 527:275–279.

Trussell GC, Lesser MP, Patterson MR, Genovese SJ (2006) Depth-specific differences in growth of the reef sponge *Callyspongia vaginalis*: role of bottom-up effects. Mar Ecol Prog Ser 323:149–158.

Vokhshoori NL, Larsen T, McCarthy MD (2014) Reconstructing 13C isoscapes of phytoplankton production in a coastal upwelling system with amino acid isotope values of littoral mussels. Mar Ecol Prog Ser 504:59–72.

Author Manuscript

Waters CN, Zalasiewicz J, Summerhayes C, Barnosky AD, Poirier C, Ga~uszka A, Cearreta A, Edgeworth M, Ellis EC, Ellis M, Jeandel C, Leinfelder R, McNeill JR, d. Richter D, Steffen W, Syvitski J, Vidas D, Wagreich M, Williams M, Zhisheng A, Grinevald J, Odada E, Oreskes N, Wolfe AP (2016) The Anthropocene is functionally and stratigraphically distinct from the Holocene. Science 351:137.

Wulff J (2017) Bottom-up and top-down controls on coral reef sponges: disentangling within-habitat and between-habitat processes. Ecology 98:1130–1139.

Author Manuscript

Figure Legends

Figure 1. Percent cover per m^2 (mean ± SE) plot of sponges at 10, 18, 30, 61 and 91 m. Regression analysis for effect of depth were all significant: *Plakortis angulospeculatus*, y=-4.0968 + 0.18922x, R^2=0.787 (*t*(28) = 8.61, P = <0.0001), *Agelas tubulata*, y=-0.1105 + 0.0054x, R^2=0.893 (*t*(28) = 6.50, P = <0.0001), *Xestospongia muta*, y=-0.7867 + 0.0305x, R^2=0.831 (*t*(28) = 8.60, P = <0.0001).

Figure 2. Bivariate plot of bulk stable isotope data for $\delta^{13}C$ and $\delta^{15}N$ from *Xestospongia muta* (Xm), *Plakortis angulospiculatus* (Plk) and *Agelas tubulata* (Agt).

Figure 3. Fingerprinting method for separating functional groups based on principal component analysis of CSIA $\delta^{13}C_{norEAA}$ data. Sponge $\delta^{13}C_{norEAA}$ values are unique, species-specific and well separated compared to potential food resources of prokaryotic and eukaryotic origin, as well as other filter feeding organisms (e.g. mussels).

Figure 4. Linear discriminant analysis plots from CSIA $\delta^{13}C_{norEAA}$ data from A) *Agelas tubulata* B) *X. muta* and C) *P. angulospiculatus.* Source end member data was taken from the Larsen et al. (2013) CSIA $\delta^{13}C_{norEAA}$ and from McMahon et al. (2016).

Figure 5. Bivariate plot of CSIA $\delta^{13}C_{EAA}$ and $\delta^{15}N_{SAA}$ stable isotope data from *Xestospongia muta* (Xm), *Plakortis angulospiculatus* (Plk) and *Agelas tubulata* (Agt).

Author Manuscript

Author Manuscript

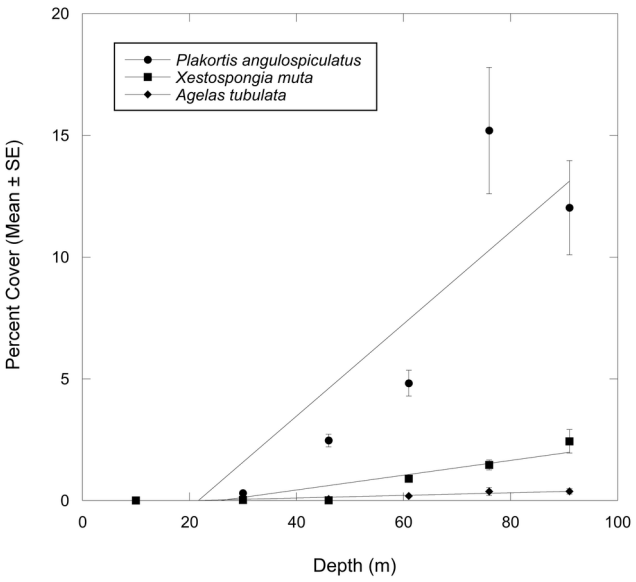

LNO_11668_Figure 1.tif

Author Manuscript

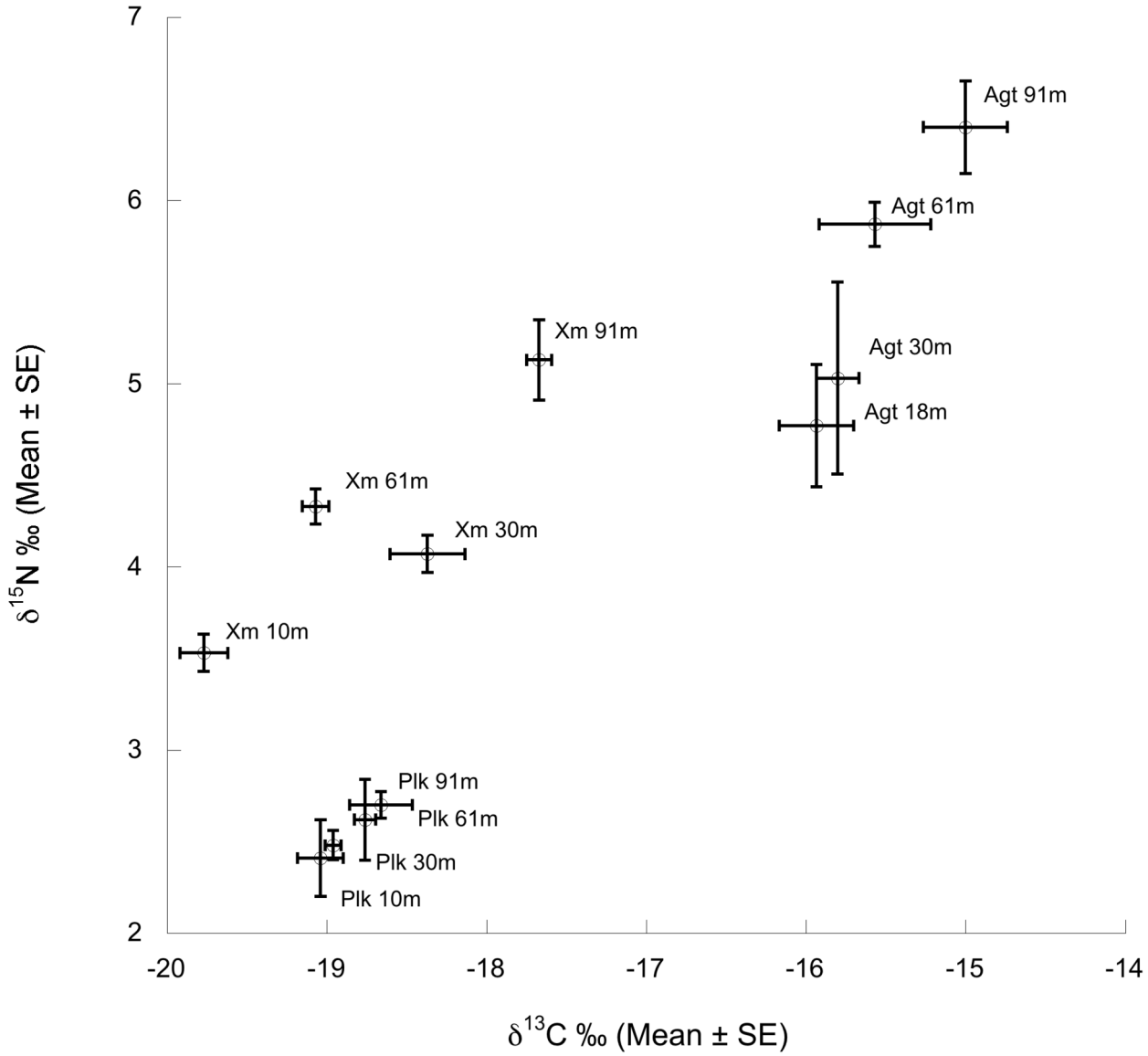

LNO_11668_Figure 2.tif

Author Manuscript

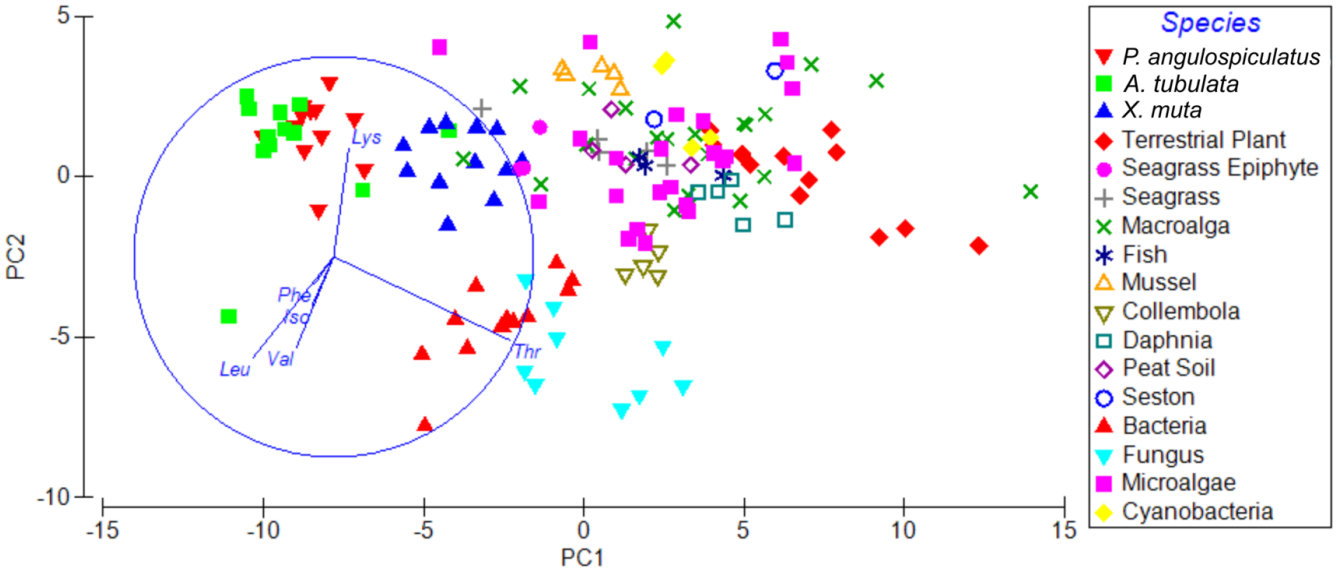

LNO_11668_Figure 3.tif

Author Manuscript

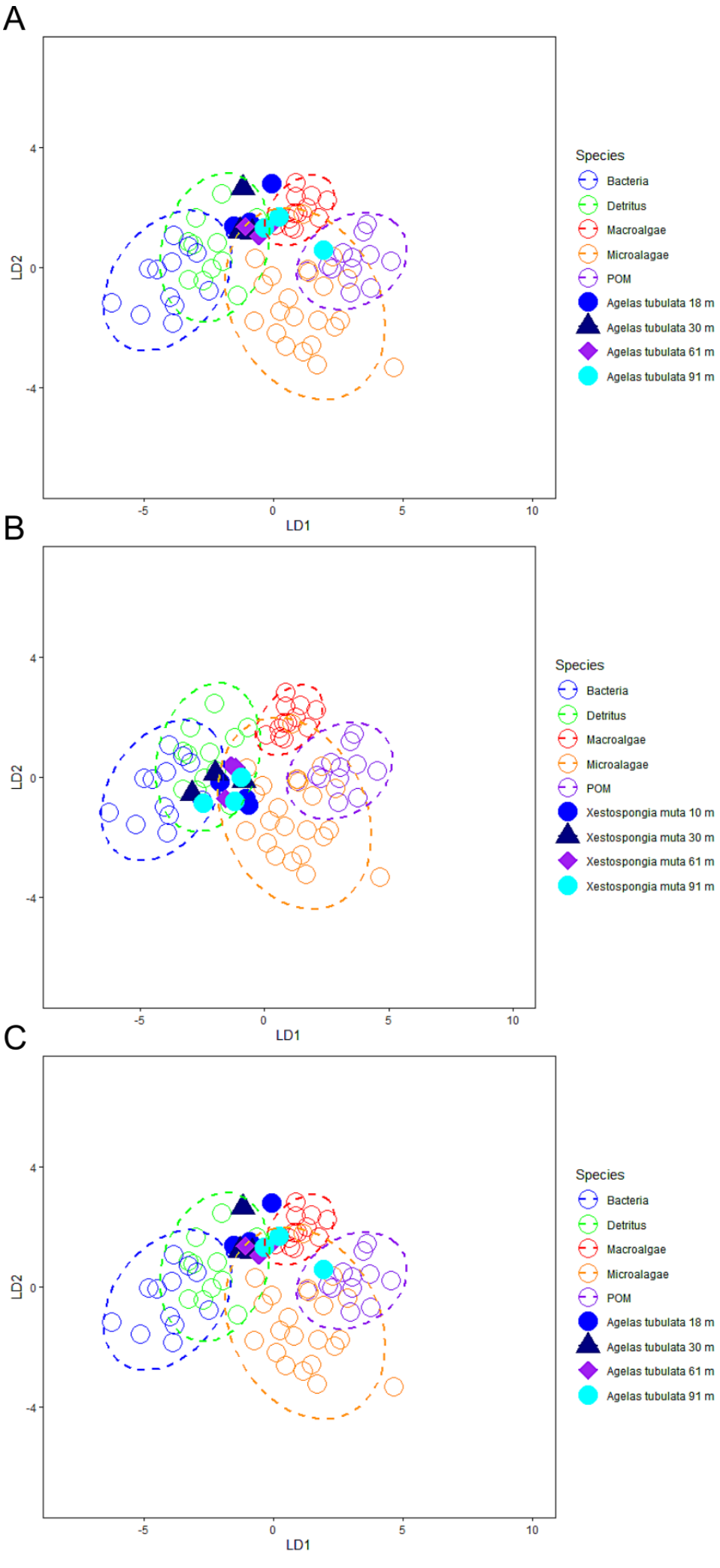

LNO_11668_Figure 4.tif

Author Manuscript

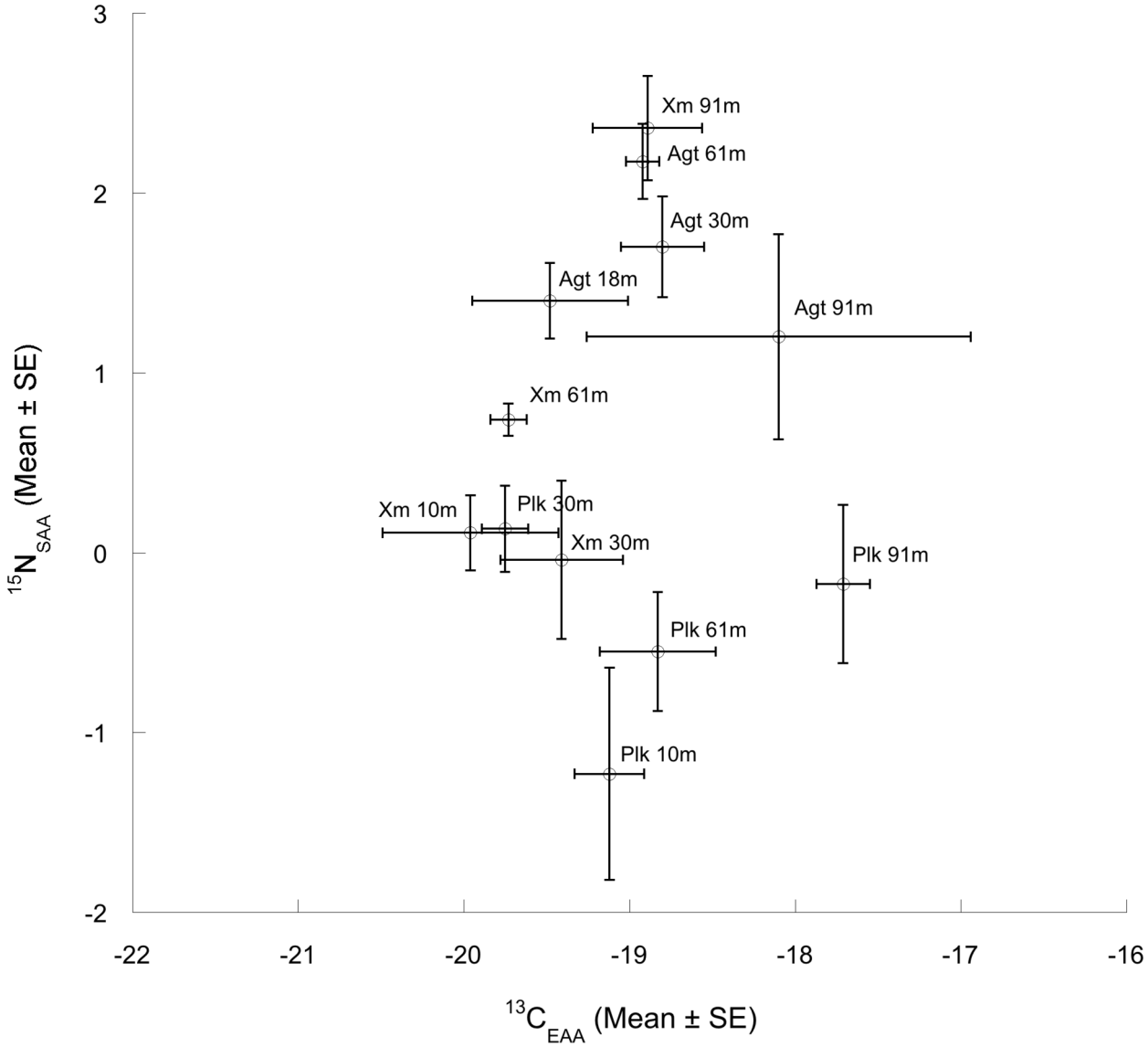

LNO_11668_Figure 5.tif